JOURNAL OF SOLID STATE CHEMISTRY 38, 87–96 (1981)

# Kinetics and Mechanistic Aspects of the Reduction of Chromium Dioxide

REGINO SAEZ-PUCHE AND MIGUEL A. ALARIO-FRANCO*

*Departamento de Química Inorgánica, Facultad de Ciencias Químicas, Universidad Complutense, Madrid 3, Spain, and Instituto de Química Inorgánica "Elhuyar," CSIC, Madrid, Spain*

Received September 2, 1980

Thermogravimetric experiments on very small, single-crystalline, acicular particles of $CrO_2$, of homogeneous size and shape, indicate that the reduction of $CrO_2$ by hydrogen to produce CrOOH, can be explained by means of a unidimensional diffusion mechanism. Hydrogen diffuses along the empty tunnels that exist parallel to the $c$ axis in the rutile-like unit cell. The corresponding diffusion equation is $D = 10^{-6}(-19.3 \pm 2.3)/RT$ cm$^2$/sec, and is valid for $490 < T < 519$ K and $30 < P_{H_2} < 110$ Torr.

## Introduction

A few years ago, Alario-Franco and Sing (*1*) demonstrated the interconversion between chromium dioxide and orthorhombic chromium oxyhydroxide, at a pressure of 1 atm, according to:

$$CrO_2 \underset{\text{Air, } O_2\ (673\ K)}{\overset{\frac{1}{2}\ H_2\ (603\ K)}{\rightleftharpoons}} CrOOH. \qquad (1)$$

The back reaction had been observed previously by Tombs *et al.* (*2*).

The facility of this interconversion process was explained (*3*) by the close analogy between the structure of both compounds: $CrO_2$, an unusual transition metal oxide which exhibits ferromagnetism (*4*) and metallic properties (*5*), has the tetragonal rutile structure, and belongs to space group $P4_2/mnm$ with $a_0 = 4.4190$ Å and $c_0 = 2.9154$ Å (*6*). On the other hand, orthorhombic CrOOH, which is paramagnetic and nonmetallic, belongs to space group $P2_1nm$, its lattice parameters being $a_0 = 4.858$ Å, $b_0 = 4.292$ Å, and $c_0 = 2.955$ Å (*7*); and can be considered as an orthorhombic distortion of the rutile structure.

From a structural point of view, the reduction of $CrO_2$ according to Eq. [1] implies the formation of hydrogen bonds between the central octahedra and the corner octahedra that, in rows parallel to the $c$ axis, build up the rutile-type structure. In this way, there is only a small rearrangement of the unit cell and there exists a close correspondence between the positions of metal and oxygen atoms in both structures (see Figs. 1a and b).

The interconversion between $CrO_2$ and CrOOH being then so simple in crystallographic terms, it was considered desirable to learn more about the dynamics of the process and we report in this paper part of

* Address all correspondence to: Laboratoire de Cristallographie, CNRS 166 X, 38042, Grenoble Cédex, France.



0022-4596/81/070087-10$02.00/0

our work on this aspect of the reduction of $CrO_2$ by hydrogen.

In general terms (*8*), gas–solid reactions are controlled either by a surface reaction or by the diffusion of the gas through the product layer which is being formed in the process. For this reason, it is important to know and, if possible, to control the surface characteristics of the reacting solid. In this connection, we were fortunate in having $CrO_2$ powders of homogeneous size and morphology and different particle dimensions.

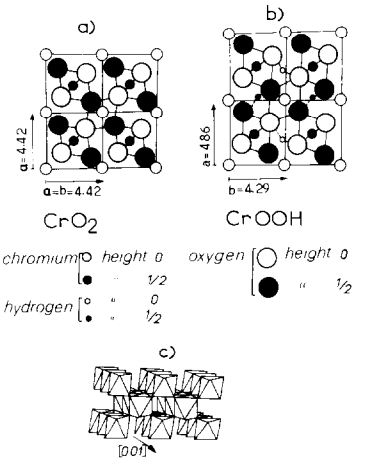


FIG. 1. (a) Projection of the rutile-type structure of $CrO_2$ along the $c$ axis of the tetragonal cell (*6*). (b) Projection of the structure of CrOOH along the $c$ axis of the orthorhombic cell (*7, 23*). (c) Perspective view of the $CrO_2$ structure showing the strings of $[MO_6]$ octahedra sharing opposite edges along the $c$ axis and the empty square tunnels parallel to it.

## Experimental

### *Materials*

The powder samples of $CrO_2$ were obtained in the RCA laboratories (USA) (*9*), by hydrothermal synthesis, and consisted of approximately prismatic nonporous particles (Fig. 2); the acicularity ratio was of the order of 10/1. Their average length, $\tau$, as determined by electron microscopy and their BET surface areas, as measured by the adsorption of nitrogen at its boiling point, were as follows (*10*):

$\tau = 0.250\ \mu m$ ($S_{BET} = 30.7\ m^2g^{-1}$);
$\tau = 0.304\ \mu m$ ($S_{BET} = 19.7\ m^2g^{-1}$);
$\tau = 0.314\ \mu m$ ($S_{BET} = 18.2\ m^2g^{-1}$);
$\tau = 0.348\ \mu m$ ($S_{BET} = 15.6\ m^2g^{-1}$);
$\tau = 0.362\ \mu m$ ($S_{BET} = 14.9\ m^2g^{-1}$);
$\tau = 0.431\ \mu m$ ($S_{BET} = 11.0\ m^2g^{-1}$).

Electron diffraction work showed that every particle was a single crystal with its longest dimension parallel to the $c$ axis of the $CrO_2$ unit cell. No impurities were detected by either X-ray or electron diffraction.

*X-Ray diffraction.* These experiments were performed on a Philips Diffractometer PW 1310 with Cu$K\alpha$ radiation; $d$ spacings were refined by a least-squares procedure, with high-purity silicon as internal standard.

*Electron microscopy and diffraction.* This work was performed on a Siemens Elmiskop 102 electron microscope, operated at 100 kV and fitted with a double tilting goniometer stage, allowing tilts of ±45° around both axes. Samples for study were ultrasonically dispersed in $n$-butanol and then transferred to holey carbon-coated copper grids.

*Reduction experiments.* In order to determine the kinetic parameters, the powder samples were reduced on a thermogravimetric apparatus based on a Cahn balance, after a design of P. Cutting (*11*). The sample temperature was measured with a chromel–chromel–alumel thermocouple placed within 5 mm of the sample pan. The precision of the temperature at the usual range of work was estimated as ±1°.

In a normal experiment, about 90 mg of


FIG. 2. Electron micrograph of the sample of $CrO_2$ with $\tau = 0.362$ μm. The acicularity ratio is of the order of 10/1 and the $c$ axis is parallel to the longest dimension.

powder was heated at the reduction temperature for 1 hr under a vacuum of $10^{-4}$ Torr. It was observed that in the course of this treatment the sample did lose a certain amount of weight. Such weight loss, see Table I, which in fact is of paramount importance in the reduction process (see below) was substracted from the initial weight before calculating the degree of the reduction, $\alpha$, according to Eq. (1). Subsequently, hydrogen of high purity (99.9995%) was introduced into the system; the hydrogen pressures used were 30, 60, 110, and 165 Torr and were measured by means of a mercury manometer; both the weight and the temperature were monitored with a two-channel recorder (Leeds and Northup, model Speedomax 682).

Thermal decomposition of the original powder samples at 900°C in air produced a

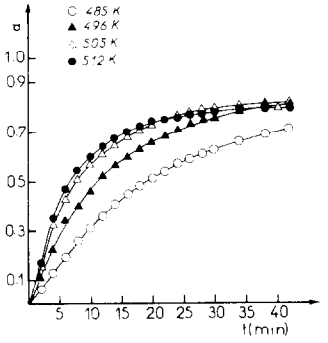


FIG. 3. Reduction isotherms for the sample with $\tau = 0.362$ μm at a hydrogen pressure of 110 Torr.

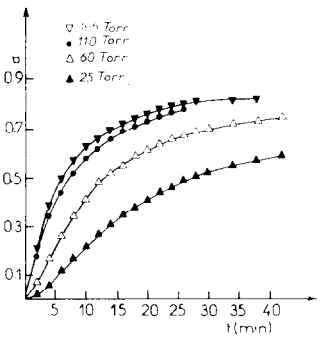


FIG. 4. Reduction isotherms for the sample with $\tau = 0.362$ μm at a temperature of 505 K.

TABLE I

RESULTS OF THE REDUCTION OF $CrO_2$ IN HYDROGEN ($P_{H_2}$ = 110 Torr)

| $T$ (K) | $\alpha_F^b$ | $P_D^c$ | $T$ (K) | $\alpha_F$ | $P_D$ |
|---|---|---|---|---|---|
| | $\tau$ = 0.250 $\mu$m[a] | | | $\tau$ = 0.348 $\mu$m | |
| 490 | 0.62 | 0.60 | 485 | 0.80 | 0.36 |
| 499 | 0.61 | 0.63 | 491 | 0.80 | 0.37 |
| 505 | 0.60 | 0.70 | 497 | 0.80 | 0.37 |
| 512 | 0.55 | 0.75 | 509 | 0.81 | 0.44 |
| 514 | 0.54 | 0.95 | 514 | 0.82 | 0.44 |
| 514 | Decomposed | 9.7 | 519 | 0.85 | 0.45 |
| | $\tau$ = 0.362 $\mu$m | | | $\tau$ = 0.431 $\mu$m | |
| 485 | 0.81 | 0.38 | 493 | 0.76 | 0.30 |
| 496 | 0.84 | 0.40 | 497 | 0.73 | 0.30 |
| 505 | 0.80 | 0.43 | 505 | 0.75 | 0.31 |
| 512 | 0.82 | 0.47 | 509 | 0.84 | 0.31 |
| 517 | Decomposed | 9.7 | 519 | 0.84 | 0.43 |

[a] $\tau$ = average particle length, see text.

[b] $\alpha_F$ = maximum final reduced state <> when slope of $\alpha/t$ curve $\simeq$ 0. $\alpha_F$ = 1 corresponds to $CrO_2 + \frac{1}{2} H_2 \rightarrow CrOOH$.

[c] $P_D$ = percent decomposition observed *in vacuo*, at the corresponding temperature, for 1 hr; 9.7% corresponds to $2CrO_2 \rightarrow Cr_2O_3 + \frac{1}{2} O_2$.

weight loss of 9.7%, in excellent agreement with the expected value for the process $2CrO_2 \rightarrow Cr_2O_3 + \frac{1}{2} O_2$.

## Results and Discussion

### (*a*) *General Kinetic Aspects*

The general outlook of the $\alpha/t$ curves for the reduction of $CrO_2$, Figs. 3 and 4 being two representative examples, corresponds closely to the usual type encountered in gas–solid reactions (*12*), although the induction period characteristic of this type of process is almost absent. It is also clear from these data that the reaction rate increases with temperature (Fig. 3) and with hydrogen pressure (Fig. 4).

The representation of these data in a reduced time plot (*13*) is a useful way for knowing the operating kinetics or, in a more rigorous way, of excluding the nonoperating paths. Figure 5 shows such a plot of our data. It can be seen that, in general terms, they fit the equation corresponding to a diffusion mechanism. The data corresponding to the samples with greater particle sizes ($\tau$ = 0.348–0.431 $\mu$m) are coincident for every value of $t/t_{0.5}$ and depart from the theoretical diffusion equation, to smaller $\alpha$ values, for $t/t_{0.5} > 2$ ($\alpha > 0.7$). However, in the case of the samples with smaller particle length ($\tau$ = 0.250–0.348 $\mu$m) our experimental points fit the theoretical curve to only $\alpha \simeq 0.5$; for higher reduced times they also deviate to smaller $\alpha$ values. This fact is more marked, the smaller the particle (Fig. 5).

Although all samples reduced were initially nonporous (*14*), they have different surface areas because of their different particle sizes. This difference is of the order of 3:1 in the extreme case (see experimental part). If the controlling path was a surface-type process we should expect differences in the reduction process and, in particular, in the reduction rates (*15*). In this connection, Table I gives a resume of the main reaction parameters. It is interesting to mention that every sample of $CrO_2$ did experience a slight decomposition in the process of establishing a constant tempera-

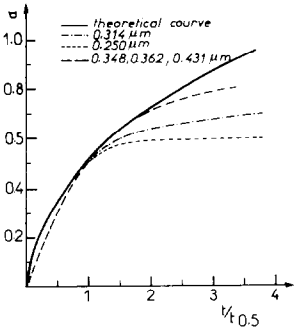


FIG. 5. Representation of the degree of reduction, $\alpha$, of $CrO_2$ in hydrogen against the reduced time $t/t_{0.5}$. Full line: calculated plot for a unidimensional diffusion equation. Dotted lines: experimental data for the different samples.

ture *in vacuo;* the amount decomposed, $P$, was greater for smaller particle length and higher temperature.

Considering the data given in Table I, it is somewhat surprising that the maximum reduction attained in the sample with the smaller particle length, $\tau = 0.250$ $\mu$m, never does exceed 62% of the value expected from the chemical equation, Eq. (1). For greater particle lengths the final states are clearly more reduced, however, they never exceed 85% of the theoretical value.

X-Ray diffraction data of the resulting products indicated, for the samples with $\tau \geq 0.348$ $\mu$m, the presence of only orthorhombic CrOOH. However, in the case of the samples with $\tau \leq 0.314$ $\mu$m, orthorhombic CrOOH coexisted with $CrO_2$. This suggests that, in those last cases, the reaction has not occurred in certain regions of the crystals. The reason of this behavior appears quite complex and is currently under investigation. We will concentrate in the following on the reduction of $CrO_2$ with particle length $\tau > 0.348$ $\mu$m.

### (*b*) *Reduction Mechanism*

In attempting to establish a mechanism for the reduction of $CrO_2$, it is worth considering its structure in some detail. As stated above, $CrO_2$ crystallizes in a rutile-type structure. An important characteristic of this structure is the presence of empty octahedra centred at the crystallographic position ($\frac{1}{2}$, 0, 0) and equivalent points. These empty octahedra form square columnar tunnels which run parallel to the $c$ axis (Fig. 1c) and are of great importance in the chemistry of rutile itself (*16*).

Although we do not know of any work on the diffusion of ions in $CrO_2$, there is a wealth of information regarding the diffusion of cations in the isostructural titanium dioxide (*17–21*). It appears from this work that this is a very anisotropic process. For example, Johnson (*17*) found that the diffusion of lithium in rutile was eight orders of magnitude faster along the $c$ axis than perpendicular to it. For most of other cations (*18*) diffusion is also anisotropic, and the proton is no exception (*19*). $Ti^{3+}$ (*20*) and $Cr^{3+}$ (*21*) are, however, exceptional in this connection: their diffusion in rutile is almost isotropic. It has been suggested by O'Keeffe and Ribble (*21*) that this fact could be related to the capability of those cations to form crystallographic shear planes (*16*).

On the other hand, it is also well known that rutile can accept a certain amount of hydrogen; it was shown by von Hippel *et al.* (*22*) that this hydrogen is located in two possible positions: joining two oxygen atoms either of the same octahedron or of different (central and corner) octahedra. In

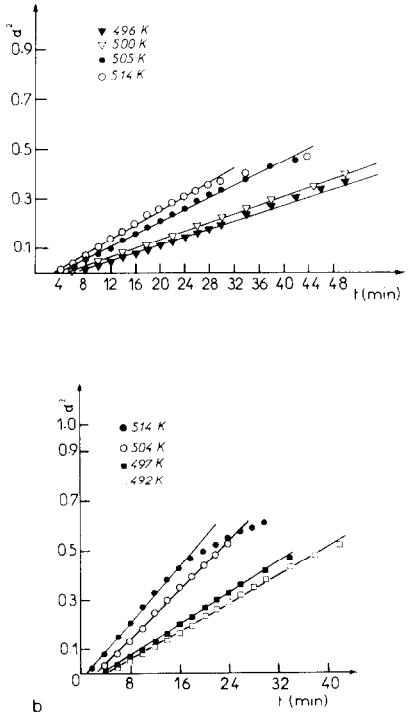


FIG. 6. Reduction isoterms plotted according to the unidimensional diffusion equation: (a) sample with $\tau = 0.348$ $\mu$m and $P_{H_2} = 110$ Torr; (b) sample with $\tau = 0.362$ $\mu$m and $P_{H_2} = 30$ Torr.

orthorhombic CrOOH, hydrogen is also bonding two oxygen atoms of different octahedra, however, as recently confirmed by a neutron diffraction study (*23*), the three bonded atoms O–H–O are on the same $x$–$y$ plane, the positions of the hydrogen atoms being located in the middle of the tunnels (see Fig. 1b).

It seems logical then to analyze the reduction of $CrO_2$ in terms of a unidimensional diffusion process by means of an interstitial mechanism along the above-mentioned tunnels. In favor of this mechanism is also the fact that the surface area of $CrO_2$ remains practically unchanged during the reduction process (*14*).

### (*c*) *Diffusion Parameters*

Considering the geometry of the particles, Fig. 2, and supposing that the diffusion of hydrogen happens parallel to their longest dimension, the solution of Fick's second law is given by the parabolic equation (*24*)

$$\alpha^2 = \frac{4Dt}{(\tau/2)^2}, \qquad (2)$$

where $t$ is the time in seconds, $\tau$ is expressed in centimeters and $D$, the diffusion coefficient, is obtained in centimeters squared per second. The representation of our data according to Eq. (2) is given, for some of the samples, on Fig. 6. It can be observed that the experimental points fit a straight line up to $\alpha = 0.7$.

The values of the diffusion coefficients obtained from the linear parts of such plots are given in Table II. It can be seen that the

TABLE II

DIFFUSION COEFFICIENTS OF HYDROGEN IN $CrO_2$

| $\tau = 0.348$ μm[a], $P_{H_2} = 110$ Torr | | $\tau = 0.362$ μm, $P_{H_2} = 110$ Torr | | $\tau = 0.431$ μm, $P_{H_2} = 110$ Torr | |
|---|---|---|---|---|---|
| $T$ (K) | $D$ ($\times 10^{14}$) ($cm^2\ sec^{-1}$) | $T$ (K) | $D$ ($\times 10^{14}$) ($cm^2\ sec^{-1}$) | $T$ (K) | $D$ ($\times 10^{14}$) ($cm^2\ sec^{-1}$) |
| 492 | 1.60 | 485 | 1.96 | 493 | 1.54 |
| 497 | 1.80 | 496 | 3.17 | 497 | 1.66 |
| 503 | 2.82 | 505 | 4.23 | 505 | 2.32 |
| 514 | 3.65 | 512 | 4.68 | 509 | 2.60 |
| | | | | 521 | 4.07 |
| $D_0 = 1.8 \times 10^{-6}\ cm^2\ sec^{-1}$ | | $D_0 = 3.4 \times 10^{-6}\ cm^2\ sec^{-1}$ | | $D_0 = 1.5 \times 10^{-6}\ cm^2\ sec^{-1}$ | |
| $E^* = 18.2$ kcal/mole | | $E^* = 18.4$ kcal/mole | | $E^* = 18.2$ kcal/mole | |
| $\tau = 0.362$ μm, $P_{H_2} = 30$ Torr | | $\tau = 0.362$ μm, $P_{H_2} = 60$ Torr | | $\tau = 0.362$ μm, $P_{H_2} = 165$ Torr | |
| $T$ (K) | $D$ ($\times 10^{14}$) ($cm^2\ sec^{-1}$) | $T$ (K) | $D$ ($\times 10^{14}$) ($cm^2\ sec^{-1}$) | $T$ (K) | $D$ ($\times 10^{14}$) ($cm^2\ sec^{-1}$) |
| 497 | 1.19 | 491 | 1.73 | 483 | 2.56 |
| 500 | 1.22 | 493 | 2.48 | 495 | 4.23 |
| 505 | 1.81 | 505 | 2.84 | 505 | 5.87 |
| 514 | 2.23 | 517 | 4.83 | | |
| $D_0 = 2.1 \times 10^{-4}\ cm^2\ sec^{-1}$ | | $D_0 = 3.2 \times 10^{-5}\ cm^2\ sec^{-1}$ | | $D_0 = 1.3 \times 10^{-6}\ cm^2\ sec^{-1}$ | |
| $E^* = 23.5$ kcal/mole | | $E^* = 20.9$ kcal/mole | | $E^* = 17.1$ kcal/mole | |

[a] $\tau$ = average particle length, see text.

diffusion coefficient of hydrogen on $CrO_2$ is, in all these samples and for all the temperatures used, at a pressure of 110 Torr of hydrogen, of the same order of magnitude: $D \simeq 10^{-14}$ $cm^2sec^{-1}$. As expected, $D$ increases with temperature. The changes in the particle length do not seem to affect very much the value of $D$, although for the sample with $\tau = 0.362$ $\mu$m, $D$ was somewhat higher (Table II). On the contrary, there seems to be a marked influence of the hydrogen pressure and the diffusion coefficient increases linearly with $P_{H_2}$ (Fig. 7). Nevertheless, we observed that for temperatures above 518 K and/or hydrogen pressures higher than 160 Torr, the reduction process was instantaneous, the resulting product being $\alpha$-$Cr_2O_3$. This suggests that, under those conditions, the operating process is

$$2CrO_2 + H_2 \xrightarrow[T = 513\ K]{P_{H_2} \geq 165\ Torr} Cr_2O_3 + H_2O. \quad (3)$$

The activation energy for diffusion, $E^*$, was obtained from an Arrhenius-type equation:

$$D = D_0 \exp(-E/RT). \quad (4)$$

The corresponding plots, which are reasonably linear, are given in Fig. 8, and allow us to obtain the $D_0$ and $E^*$ values which appear in Table II.

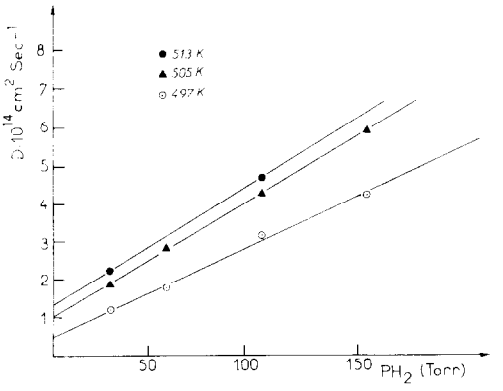


FIG. 7. Influence of the hydrogen pressure on the diffusion coefficient in the reduction of $CrO_2$. Sample with $\tau = 0.362$ $\mu$m.

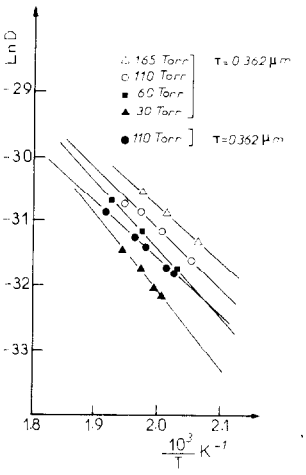


FIG. 8. Arrhenius-type plot for the diffusion of hydrogen in $CrO_2$ with different particle sizes at different hydrogen pressures.

It can be observed that the activation energy for a constant hydrogen pressure (110 Torr) is practically independent of particle size, and amounts to 18.2 kcal/mole. This seems to be a clear confirmation that the surface reaction plays no role in controlling the kinetics. It is worth recalling in this connection (see Experimental) that the ratio of the surface areas of the samples with $\tau = 0.348$ $\mu$m and $\tau = 0.431$ $\mu$m was 1.4.

On the other hand, for a constant particle size, $\tau = 0.362$ $\mu$m, $E^*$ decreases with the increase in the hydrogen pressure (Table II). This is also in agreement with a diffusion-controlled reaction, since more hydrogen will be able to enter the tunnels when the pressure increases.

The average activation energy for the reduction of $CrO_2$ from all our experiments is $E^* = 19.3$ kcal/mole with a standard deviation of 2.3 kcal/mole. This is considerably lower than the value given by Hill (25) for the diffusion of protons in rutile, 50.9 kcal/mole, and somewhat higher than the more recent data reported by Johnson

(*26*) for the diffusion of both hydrogen and deuterium in $TiO_2$ along the $c$ axis. The actual values given by Johnson *et al.* were $E^* = 13.6$ and $= 29$ kcal/mole for the diffusion of hydrogen parallel and perpendicular to the $c$ axis, respectively (*26*).

Our results seem then to suggest that the reduction of $CrO_2$ by hydrogen happens by a direct interstitial diffusion mechanism. The direction of diffusion is probably parallel to the $c$ axis which coincides with the particle longest dimension (see experimental part above). However, the diffusion of hydrogen in rutile is faster than in $CrO_2$ for the same temperature, a fact reflected in the much smaller preexponential factors, $D \simeq 10^{-6}$, obtained in our work (Table II).

According to random-walk theory (*27*) the average displacement of an atom in a diffusion process $(\bar{R}_n^2)^{1/2}$ is proportional to the square root of the number of jumps $n$.

$$(\bar{R}_n^2)^{1/2} = dn, \tag{5}$$

where $d$ is the jump distance. On the other hand, the jump frequency, $F$, is related to the diffusion coefficient by an expression analogous to Fick's first law:

$$D = \tfrac{1}{2}d^2F. \tag{6}$$

In the case of $CrO_2$, for the average temperature of our experiments, 550 K, and a jump distance equal to the $c$ parameter of the unit cell ~3 Å, the jump frequency is 29.3 $sec^{-1}$ and the average displacement $(\bar{R}_n^2)^{1/2} = 1.6 \times 10^{-7}$ cm $sec^{-1}$.

As the dimensions of our crystals are of the order of 4000 Å the reaction should be complete for the reaction times used in our experiments, i.e., 40 min. However, as noted above, the reaction final state is never higher than $\alpha = 0.85$.

In the case of rutile, for comparable temperatures $F = 5.5 \times 10^{-6}sec^{-1}$ and $(\bar{R}_n^2)^{1/2} = 7 \times 10^{-5}$ cm $sec^{-1}$. It is worth pointing out, however, that the hydrogen reduction of $TiO_2$ gives rise to a very different product, $Ti_3O_5$ (*28*), and not TiOOH; the kinetics of this process are also different (*29*).

In a diffusion process, the activation energy, which is equal to the difference in energy between the ground state and the saddle point (*30*), is, in fact, composed of two terms:

$$E^* = E_F^* + E_M^*, \tag{7}$$

where $E_F^*$ is the energy needed to create the carrier and $E_M^*$ the activation energy for its movement. Considering that in orthorhombic CrOOH the hydrogen atoms are bonded to two oxygen atoms one from a central octahedron and another from a corner octahedron (see Fig. 1b), one can imagine that, once the hydrogen has been fixed in a normal position at the tunnel entrance, this hydrogen bond must be broken for the hydrogen to move to the next normal position. In other words, the energy for the carrier formation must be close to the hydrogen bond energy. A neutron diffraction study of orthorhombic CrOOH (*23*), indicates that the hydrogen bond is asymmetric and nonlinear, and has the following distances: $\delta_{O-H} = 1.408$ Å to an oxygen of the central octahedron and $\delta_{O-H} = 1.168$ Å to an oxygen of the corner octahedron. On the other hand, the distance between those two oxygen atoms is $\delta_{O-O} = 2.550$ Å. According to Lippincot and Schroeder (*31*) there is a correlation between the O–O distance on a hydrogen bond and the bond energy. In this correlation, a distance of $\delta_{O-O} = 2.550$ Å corresponds to a bond energy of 10.7 kcal/mole. Nevertheless, the Lippincot and Schroeder plot applies to linear hydrogen bonds, while, in our case, the hydrogen bond is bent. If we then consider the oxygen–oxygen distance, $\delta_{O-O}$, as the sum of the two $\delta_{O-H}$ distances, $\delta'_{O-O} = 2.576$ Å: a hydrogen bond energy of 9.4 kcal/mole results. In any event, as the total activation energy for diffusion obtained in the present work is 19.3 kcal/mole, it would appear

that the activation energy of migration, $E_M^*$, is about 9 kcal/mole.

### (*d*) *Concluding Remarks*

The kinetics of the hydrogen reduction of $CrO_2$ to CrOOH seem then to be well accounted for by a direct interstitial mechanism along the tunnels parallel to the *c* axis. The activation energy of such a process, 19 kcal/mole, appears to be shared about equally between the energy needed to create the carrier and that required for its migration.

Interestingly enough, in boehmite, which has a very different structure (*32*), the hydrogen bond energy estimated from the Lippincot and Schroeder plot is about 6 kcal/mole, while the activation energy of proton diffusion is about 13 kcal/mole (*31*). Again both terms have about the same energy.

There are still some unresolved aspects of the hydrogen reduction of $CrO_2$; among them a crucial issue seems to be the influence of the predecomposition of $CrO_2$ on its subsequent reduction. Work on these problems is in progress in our laboratory.

## Acknowledgments

We thank Dr. Hockings (RCA Laboratories, USA) for providing the samples, Professor K.S.W. Sing (Brunel University, U.K.) for encouragement, and Dr. J. Müller (Laboratoire de Cristallographie CNRS, Grenoble) for valuable discussions.

## References

1. M. A. Alario-Franco and K. S. W. Sing, *J. Thermal Anal.* **4**, 47 (1972).
2. N. C. Tombs, W. J. Croft, J. R. Carter, and J. F. Fitzgerald, *Inorg. Chem.* **3**, 1791 (1964).
3. M. A. Alario-Franco, J. Fenerty, and K. S. W. Sing, *in* Proceedings of the 7th International Symposium on the Reactivity of Solids" (Bristol, 1972; J. S. Anderson, M. W. Roberts, and F. S. Stone, Eds.), p. 327, Plenum, New York (1973).
4. L. Blanc, *Ann. Chim.* **6**, 217 (1926).
5. B. Kubota and H. Hirota, *J. Phys. Soc. Japan* **16**, 345 (1960).
6. P. Porta, M. Marezio, J. P. Remeika, and P. C. Dernier, *Mater. Res. Bull.* **7**, 157 (1972).
7. A. N. Christensen, *Inorg. Chem.* **5**, 1542 (1966).
8. J. Szekely, J. W. Evans, and H. Y. Sohn, "Gas Solid Reactions," chap. 1, Academic Press, New York (1976).
9. J. P. Dismukes, D. F. Martin, L. Ekstrom, C. C. Wang, and M. D. Coults, *Ind. Eng. Chem. Proc. Res. Develop.* **10**(3), 319 (1971).
10. R. Saez-Puche, Ph. D. Thesis, Universidad Complutense, Madrid (1979).
11. P. A. Cutting, Ph. D. Thesis, Brunel University (1970).
12. A. K. Galwey, "The Chemistry of Solids," chap. 5, Chapman & Hall, London (1967).
13. J. H. Sharp, G. W. Brindley, and B. N. Narahari-Achar, *J. Amer. Ceram. Soc.* **49**, 379 (1966).
14. M. A. Alario-Franco and K. S. W. Sing, *in* "Pore Structure and Properties of Materials" (Proceedings of the International Symposium, Prague, 1973; S. Modry, Ed.), p. B-107, Akademia, Prague (1974).
15. B. Delmon, "Introduction a la Cinétique Hétérogène," chap. 3, Editions Technipress, Paris (1969).
16. L. A. Bursill and B. Hyde, *Progr. Solid State Chem.* **7**, 5 (1972).
17. O. W. Johnson, *Phys. Rev. A* **136**, 284 (1964).
18. J. P. Wittke, *J. Electrochem. Soc.* **113**(2), 193 (1966).
19. J. W. de Ford and O. W. Johnson, *J. Appl. Phys.* **46**(3), 1013 (1975).
20. T. S. Lundy and W. A. Coghlan, *J. Phys.* **34**(11–12), Suppl. C-9, 299 (1973).
21. M. O'Keeffe and J. J. Ribble, *J. Solid State Chem.* **4**, 351 (1972).
22. A. Von Hippel, J. Kalnays, and W. B. Weaphal, *J. Phys. Chem. Solids* **23**, 779 (1962).
23. M. Pernet, C. Berthet-Colominas, M. A. Alario-Franco, and A. N. Christersen, *Phys. Status Solidi* **43**, 81 (1977).
24. W. Jost, "Diffusion in Solids," chap. 1, Academic Press, New York, (1960).
25. G. J. Hill, *Brit. J. Appl. Phys.* **21**, 1151 (1968).

26. O. W. JOHNSON, S. H. PAK, AND J. W. DE FORD, *J. Appl. Phys.* **46**(3), 1026 (1975).
27. P. G. SHEWMON, "Diffusion in Solids," chap. 2, McGraw–Hill, London (1963).
28. P. EHRLICH, *Z. Elektrochem.* **45,** 362 (1939).
29. T. IWAKI, M. KOMURO, K. HIROSAWA, AND M. MIURA, *J. Catal.* **39,** 324 (1975).
30. R. F. BREBRICK, *in* "Solid State Physics and Chemistry," (P. F. Weller, Ed.), chap. 9, p. 602, Chapman & Hall, London (1974).
31. E. R. LIPPINCOTT AND R. SCHROEDER, *J. Chem. Phys.* **23**(6), 1099 (1955).
32. F. J. EWING, *J. Chem. Phys.* **3,** 420 (1935).
33. A. MATA ARJONA AND J. J. FRIPIAT, *J. Chem. Soc. Faraday Trans.* **63,** 236 (1967).